ORIGINAL ARTICLE

Homoectoine Protects Against Colitis by Preventing a Claudin Switch in Epithelial Tight Junctions

Karla F. Castro-Ochoa[1] · Hilda Vargas-Robles[1] · Sandra Chánez-Paredes[1] · Alfonso Felipe-López[1,6] · Rodolfo I. Cabrera-Silva[1] · Mineko Shibayama[2] · Abigail Betanzos[2,3] · Porfirio Nava[4] · Erwin A. Galinski[5] · Michael Schnoor[1]

Abstract

Background Inflammatory bowel diseases (IBD) are multifactorial disorders affecting millions of people worldwide with alarmingly increasing incidences every year. Dysfunction of the intestinal epithelial barrier is associated with IBD pathogenesis, and therapies include anti-inflammatory drugs that enhance intestinal barrier function. However, these drugs often have adverse side effects thus warranting the search for alternatives. Compatible solutes such as bacterial ectoines stabilize cell membranes and proteins.

Aim To unravel whether ectoine (1,4,5,6-tetrahydro-2-methyl-4-pyrimidinecarboxylic acid) and homoectoine (4,5,6,7-tetrahydro-2-methyl-1H-(1,3)-diazepine-4-carboxylic acid), a synthetic derivative of ectoine, have beneficial effects during dextran sulfate sodium (DSS)-induced colitis in mice.

Methods/Results We found that the disease activity index was significantly reduced by both ectoines. DSS-induced edema formation, epithelial permeability, leukocyte recruitment and tissue damage were reduced by ectoine and homoectoine, with the latter having stronger effects. Interestingly, the claudin switch usually observed during colitis (decreased expression of claudin-1 and increased expression of the leaky claudin-2) was completely prevented by homoectoine, whereas ectoine only reduced claudin-2 expression. Concomitantly, only homoectoine ameliorated the drop in transepithelial electrical resistance induced by IFN-γ and TNF-α in Caco-2 cells. Both ectoines inhibited loss of ZO-1 and occludin and prevented IFN-γ/TNF-α-induced increased paracellular flux of 4 kDa FITC-dextran in vitro. Moreover, both ectoines reduced expression of pro-inflammatory cytokines and oxidative stress during colitis.

Conclusion While both ectoine and homoectoine have protective effects on the epithelial barrier during inflammation, only homoectoine completely prevented the inflammatory claudin switch in tight junctions. Thus, homoectoine may serve as diet supplement in IBD patients to reach or extend remission.

Keywords Ectoine · Intestinal permeability · Tight junction · Pro-inflammatory cytokines · Dextran sulfate sodium

Abbreviations

AJ	Adherens junction
APJ	Apical junction complex
CD	Crohn's disease
DAI	Disease activity index
DSS	Dextran sulfate sodium
IBD	Inflammatory bowel diseases
IFN-γ	Interferon-γ
IL	Interleukin
KO	Knock-out
MPO	Myeloperoxidase
ROS	Reactive oxygen species
TEER	Transepithelial electrical resistance
TJ	Tight junction
TNBS	2,4,6-Trinitrobenzenesulfonic acid
TNF-α	Tumor necrosis factor alpha
UC	Ulcerative colitis
ZO	Zonula occludens

✉ Michael Schnoor
  mschnoor@cinvestav.mx

Extended author information available on the last page of the article

Introduction

Inflammatory bowel diseases (IBD) are complex inflammatory disorders of the intestines comprising ulcerative colitis (UC) and Crohn's disease (CD). CD causes a transmural inflammation, affects any part of the gastrointestinal tract in a discontinuous pattern, and is associated with complications like granulomas, fistulas and strictures. UC is a confined inflammation of the colonic mucosa affecting mainly the rectum and the distal colon in a continuous manner [1, 2]. In both forms of IBD, a chronic and recurrent inflammation is caused in part by an uncontrolled immune response to the antigens of the intestinal microflora [1]. The specific etiology is still unknown, but it is commonly accepted that IBD has multifactorial causes including epithelial barrier disruption. The intestinal epithelial barrier controls the passage of nutrients, water and electrolytes, meanwhile impeding the passage of pathogens and toxins. It is composed of a layer of mucins produced by specialized epithelial cells termed goblet cells; and the epithelium itself which is formed by a monolayer of epithelial cells sealed between adjacent epithelial cells by the apical junction complex (AJC). The AJC regulates the passage of ions and macromolecules [3] and is therefore critical for controlling intestinal permeability, which is increased in IBD. While increased permeability is not sufficient to induce colitis [4], it can significantly aggravate the symptoms of IBD patients. Currently, therapies exist that aim at ameliorating the inflammatory response, balancing the microbiota or suppressing the proliferation of immune cells [5]. Unfortunately, many of the drugs cause severe adverse effects such as metabolic syndrome in the case of corticosteroids, and increased risk of opportunistic infections with TNF-α antibodies [6]. Thus, the search for alternative approaches is a priority.

Ectoine (1,4,5,6-tetrahydro-2-methyl-4-pyrimidinecarboxylic acid, Fig. 1a) is a compatible solute produced by extremophilic microorganisms that accumulate it in the cytoplasm to protect their biomolecules from denaturation caused by the extreme environments in which they live [7].
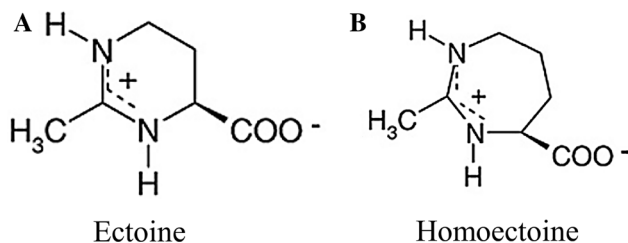
It maintains the integrity of proteins, membranes, nucleic acids as well as whole cells by stabilizing the hydration shell of biomolecules without interfering with essential cellular processes and metabolism [8, 9]. Ectoine has an anti-inflammatory effect in the skin damaged by UV-light by preventing the release of ceramides which activate the transcription factor AP-2 and expression of pro-inflammatory genes [10]. In the lung, ectoine ameliorates inflammation induced by carbon nanoparticles by reducing the number of recruited neutrophils and the production of pro-inflammatory cytokines [11]. Ectoine has also protective effects during experimental colitis in rats; however, the underlying mechanisms still remain elusive [12]. Homoectoine (4,5,6,7-tetrahydro-2-methyl-1H-(1,3)-diazepine-4-carboxylic acid, Fig. 1b) is a synthetic ectoine derivative that has stronger stabilizing effects on nucleic acids and polymerases compared to ectoine [13]. However, potential protective effects of homoectoine in other systems have not been studied.

In this study, we analyzed the effects of ectoine and homoectoine on the maintenance of intestinal epithelial barrier integrity during DSS-induced colitis. We demonstrate that these compounds ameliorate DSS-induced intestinal epithelial barrier dysfunction by stabilizing junction architecture, and by decreasing inflammation, leukocyte infiltration and oxidative stress.

Methods

Reagents and Antibodies

Dextran sulfate sodium (DSS; 40–50 kDa) was purchased from Affymetrix (Cleveland, OH). Ectoine was extracted and purified from *Halomonas elongata* DSM 2581 by bacterial milking as previously described [14]. Homoectoine was chemically synthesized from L-ornithine according to published protocols [15]. Occult bleeding was analyzed using the ColoScreen kit (Helena Laboratories, TX) according to the manufacturer's instructions. The following antibodies were used: anti-ZO-1, anti-occludin, anti-claudin-1, anti-claudin-2, Alexa Fluor secondary antibodies (Thermo Fisher, Mexico City), anti-E-cadherin and anti-β-catenin (Santa Cruz Biotechnologies, Santa Cruz, CA).

Cell Culture

The human epithelial colorectal adenocarcinoma cell line Caco-2 was obtained from ATCC (Manassas, VA) and cultured according to the provided protocols.

Fig. 1 Chemical structure of the compatible solutes. **a** Ectoine (1,4,5,6-tetrahydro-2-methyl-4-pyrimidinecarboxylic acid) and **b** Homoectoine ((S)-4,5,6,7-tetrahydro-2-methyl-1H-(1, 3)-diazepine-4-carboxylic acid)

Transepithelial Electrical Resistance (TEER) and FITC-Dextran Paracellular Flux Measurements

Caco-2 cells were cultured on 0.4-µm pore size transwell filters (Corning, Monterrey, Mexico). TEER was measured every 24 h for 7 days using a Millicell-ERS2 Volt-Ohm Meter (Millicell ERS; Millipore Co., Bedford, MA). Once confluent, cells were incubated in the presence or absence of homoectoine or ectoine (1 mM), in both upper and lower transwell chambers, in parallel to IFN-γ (100U/ml) and TNF-α (5 nM) administration.

For paracellular flux measurements, 10 µl of 4 kDa FITC-Dextran (10 µg/µl) was added to the apical compartment of monolayers when differences in TEER were measured. After 24 h, 100 µl of the basolateral medium was collected, replaced with 100 µl fresh medium and the fluorescence was measured at an excitation/emission wavelength of 492/520 nm.

Mice, DSS-Colitis and Treatment

Adult male C57BL/6 mice, weighing 20–25 g were used in colitis experiments. All experiments have been approved by the Institutional Animal Care and Use Committee of Cinvestav. All animals had ad libitum access to standard pellet diet and water over the entire experimental period of 7 days. The colitis group received 3.5% DSS in drinking water. The colitis + treatment groups were gavage-fed once daily with 100 mg/kg homoectoine or ectoine in water as previous studies have shown that this dose was the most efficient to ameliorate inflammation [16]. The control + treatment groups received normal drinking water and the same daily dose of homoectoine or ectoine. The disease activity index (DAI) consisting of weight loss, stool consistency and intestinal bleeding was determined daily as described [17]. After 7 days, animals were sacrificed by cervical dislocation; colons were removed, measured and then used in further experiments.

In Vivo Intestinal Epithelial Permeability

Animals were anaesthetized by intraperitoneal injection of ketamine/xylazine (100 mg/kg and 13 mg/kg of body weight, respectively) in 0.9% saline solution. A laparotomy was performed; the colon was exposed and a small polyethylene tube (G22) was inserted into the colon *ascendens* immediately adjacent to the cecum. The colon was cleaned thoroughly with PBS followed by instillation of 1.5% Evans blue (960.81 g/mol (Dalton)) solution and incubation for 15 min. Mice were euthanized by cervical dislocation, colons removed, rinsed with abundant PBS and washed with 1 ml of 6 mM N-acetylcysteine in PBS to eliminate excess dye. Colon was weighted, and leaked dye was extracted

overnight at RT in 2 ml of N,N dimethylformamide. Dye concentration in the supernatant was determined spectrophotometrically at 610 nm.

Histology

Colon cross-sections embedded in Tissue-Tek O.C.T. Compound (Sakura, Torrance, CA) and mounted on glass slides were stained with hematoxylin and eosin using standard protocols. Histological inflammation score was determined by degree of inflammation, extent of inflammation and crypt damage in relation to the percentage of epithelium involved in each slide as previously reported [17].

Immunofluorescence Staining

Colon cryo-sections were mounted on glass slides, fixed in 100% ethanol for 30 min at − 20 °C, washed with PBS, and blocked at 4 °C overnight in 1X PBS containing 0.01% Tween and 2% bovine serum albumin (BSA, Sigma-Aldrich). Colon sections were incubated overnight at 4 °C in primary antibodies diluted in PBS. Slides were washed and then incubated for 2 h with Alexa Fluor 488-labeled species-specific secondary antibodies. Cover slips were mounted in ProLong Gold Antifade Mountant with DAPI (Thermo Fisher Scientific) and analyzed using a confocal laser microscope (Leica TCS SPE, Leica Microsystems, Germany).

Fluorescence Microscopy of Oxidative Stress

Colon cryo-sections on glass slides were incubated with 5 µM dihydroethidium (DHE, Life Technologies, Grand Island, NY) in water at 37 °C for 30 min in the dark as previously described [18]. Fluorescence of oxidized ethidium was determined using a laser confocal microscope.

RT-PCR

Total RNA was isolated from colon tissues of three independent mice per group using Trizol reagent (Invitrogen, Carlsbad, CA) according to the manufacturer's instructions. RNA was subsequently purified by LiCl precipitation to remove DSS [19]. cDNA was synthetized using Superscript II reverse transcriptase and oligo-$(dT_{12–18})$ primers (Invitrogen). PCR was performed independently on all samples ($n = 3$ per group) using Taq-DNA polymerase (Roche, Indianapolis, IN) on a Veriti 96-well thermal cycler (Applied Biosystems, Mexico City, Mexico). The following primers were used: KC-FW: 5′–TGTCAGTGCCTGCAGACCAT–3′ and KC-RV: 5′–CCT GAGGGCAACACCTTCA–3′; IL1β-FW: 5′-GCAACTGTT CCTGAACTCAACT– 3′and IL1β-RV: 5′-TCTTTTGGG GTCCGTCAACT–3′; IL10-FW: 5′-ACTGCACCCACT

TCCCAGT – 3´ and IL10-RV: 5´-TGTCCAGCTGGTCCT TTGTT–3´; IFNγ-FW 5´-TCAAGTGGCATAGATGTG GAA–3´ and IFNγ-RV 5´-TGGCTCTGCAGGATTTTC ATG–3´; TNFα-FW 5´-ACGGCATGGATCTCAAAGAC-3´ and TNFα-RV 5´-AGATAGCAAATCGGCTGACG-3´; βactin-FW 5´-TATCCACCTTCCAGCAGATGT-3´ and βactin-RV 5´-AGCTCAGTAACAGTCCGCCTA-3´; Mucin-2-FW: 5´-ACCTGGAAGGCCCAATCAAG-3´; Mucin-2-RV: 5´-CAGCGTAGTTGGCACTCTCA-3´. PCR conditions for KC and IL-1β were: 94 °C for 2 min, 30 cycles of 94 °C for 30 s, 55 °C for 30 s, 72 °C for 30 s, and a final extension at 72 °C for 10 min. PCR conditions for IFN-γ, TNF-α, IL-10 and MUC2 were: 94 °C for 2 min, 35 cycles of 94 °C for 30 s, 55 °C for 30 s, 72 °C for 30 s, and a final extension at 72 °C for 10 min. Amplicons were analyzed by 1.5% agarose gel electrophoresis, and shown in an inverted black-and-white manner (Fig. 6a, representative images are show). Quantification of band pixel intensities was performed using ImageJ software, and statistical analysis was performed using GraphPad Prism software v5.0 software.

Western Blot

RIPA tissue lysates were separated in 8% SDS-PAGE (15% in case of claudins) for 2 h at 120 V and transferred to a nitrocellulose membrane. Membranes were blocked with TBST containing 5% skim milk for 1 h at room temperature and incubated overnight in primary antibodies at 4 °C with gentle agitation. Membranes were washed with TBST 3 times for 10 min each and incubated with species-specific secondary antibodies conjugated to horseradish-peroxidase for 1 h at room temperature with gentle agitation. After another 3 washes for 10 min each, signals were developed using SuperSignal West Pico (ThermoFisher Scientific) and imaged on a ChemiDoc (Bio-Rad). Pixel density was quantified using ImageJ software.

Statistics

Data are represented as the mean ± standard error (SEM) or standard deviation (SDM) of the mean. The significance between groups was assessed by Student's t test or ANOVA where appropriate. Analysis was performed using GraphPad Prism software v5.0. Values of probability $(P) < 0.05$ were considered statistically significant.

Results

Homoectoine and Ectoine Attenuate DSS-Induced Colitis

Ectoine is a compatible solute with anti-inflammatory properties in different in vitro and in vivo models [10, 16, 20, 21]. Homoectoine is a synthetic derivate whose properties are still largely unknown. Thus, we tested whether homoectoine and ectoine had similar effects on the clinical progression of colitis. Mice suffering from acute colitis present three characteristic clinical signs: severe diarrhea, intestinal bleeding and significant weight loss that can be determined as disease activity index (DAI) [17]. As expected, administration of ectoine and homoectoine alone did not affect any of the investigated parameters (Fig. 2), with the score remaining at 0 during the entire course of the experiment in the untreated control group. By contrast, mice receiving DSS had a progressive DAI increase reaching a maximum score of 11.09 ± 0.61 after seven days. Both homoectoine and ectoine significantly reduced the DAI beginning 5 days after DSS treatment. However, we observed stronger protective effects on intestinal bleeding (Fig. 2b) and stool consistency (Fig. 2c) than on weight loss (Fig. 2d).

Homoectoine and Ectoine Reduce DSS-Induced Edema Formation, Leukocyte Influx, Permeability and Tissue Damage

We analyzed tissue morphology by hematoxylin and eosin staining of colon cross-sections to determine how homoectoine and ectoine protect against colitis progression. Homoectoine and ectoine treatment alone did not affect tissue morphology (data not shown). Mice with DSS-colitis showed severe edema formation, leukocyte infiltration, apical erosion and loss of intestinal crypts (Fig. 3a). Homoectoine and ectoine-treated colitic mice only showed moderate tissue damage with the surface epithelium remaining largely intact (Fig. 3a). Intestinal crypt shortening was strongly reduced, and edema formation was completely prevented. However, some areas with leukocyte infiltration could still be observed. Furthermore, a high proportion of goblet cells were observed in the colon of mice co-treated with homoectoine and ectoine, despite the induction of acute colitis which usually reduces the number of goblet cells [22].

A histological inflammation score was obtained by determining the degree of inflammation, inflammation extent and crypt damage as previously reported [17]. Both compatible solutes significantly reduced the histological inflammation score (Table 1). Interestingly, homoectoine reduced inflammation and the extent of inflammation and crypt damage more efficiently than ectoine.

Given the observed beneficial effects on colon histology, we analyzed the shortening of the entire colon, which is also a characteristic feature of colitis caused by submucosal edema and muscularis hypertrophy. Compared with the healthy group, colons of DSS-treated mice were significantly shortened by 27.92%. Of note, colon lengths of colitic mice treated with homoectoine or ectoine were significantly less
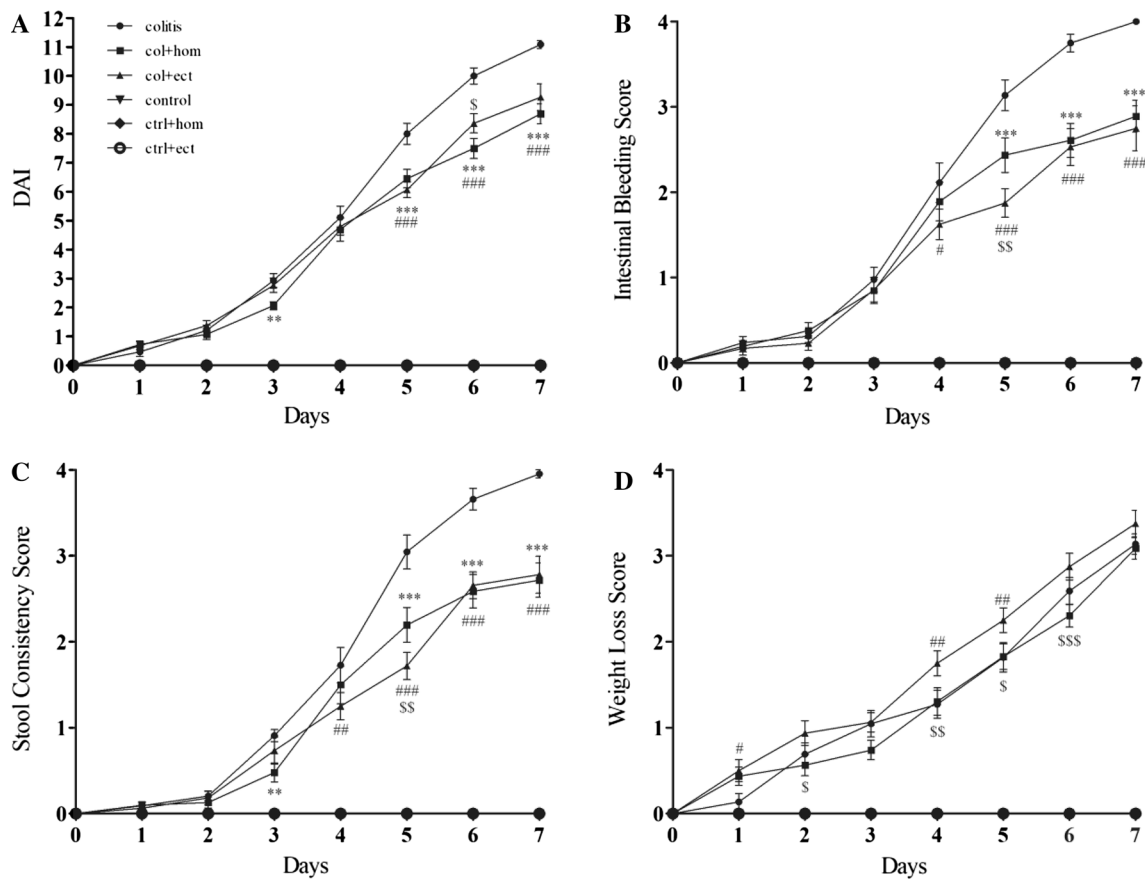
Fig. 2 Homoectoine and ectoine protect against severe colitis. **a** Both compatible solutes reduce the overall disease activity index (DAI) of DSS-induced colitis. However, different effects on the single DAI parameters intestinal bleeding (**b**), stool consistency (**c**) and weight loss (**d**) were observed. Control groups that received either water ($n = 6$), homoectoine ($n = 4$) or ectoine ($n = 4$) maintained a score of 0 during the entire course of the experiment. DAI of colitic mice co-treated with homoectoine ($n = 10$) or ectoine ($n = 11$) were significantly lower after 5–7 days compared to mice treated with DSS alone ($n = 8$). Values are displayed as mean ± standard deviation of the mean (SDM). ***$p < 0.001$, **$p < 0.01$ and *$p < 0.05$. *colitis vs col + hom; # colitis vs col + ect; $ col + hom vs col + ect

shortened with no significant difference between both treatments (Fig. 3b).

Then, we measured changes in colon permeability in vivo using Evans Blue to determine epithelial barrier integrity in the colon (Fig. 3c). As expected, permeability significantly increased in DSS-treated mice in comparison with healthy controls. Evans blue uptake in DSS-treated mice that received either homoectoine or ectoine was not only completely prevented, but even lower than in the control group. Together, these data clearly show an overall protective effect of both ectoine and homoectoine on tissue morphology and intestinal epithelial barrier integrity.

Junction Architecture Is Better Preserved by Homoectoine During DSS-Colitis

Intestinal permeability is in large part regulated by the AJC. Thus, we investigated junction architecture. The effect of homoectoine and ectoine on the expression and distribution of tight junctions (TJ) and adherens junctions (AJ) proteins during DSS-induced colitis was determined by western blotting (WB) and immunofluorescence stainings (IFs). The TJ proteins ZO-1 and occludin were significantly downregulated during DSS-induced colitis, as expected. Importantly, both homoectoine and ectoine prevented this downregulation of ZO-1 and occludin (Fig. 4a). IFs showed that both ZO-1 and occludin were reduced at cell contacts during colitis (Fig. 4b). In colitic mice treated with homoectoine or ectoine, localization of both ZO-1 and occludin was maintained at cell contacts, with homoectoine preserving the junctional localization even better.

Claudins play an important role in barrier function. Claudin-1 has a sealing function, whereas claudin-2 forms paracellular channels promoting permeability of ions [23]. Thus, we analyzed claudin-1 and claudin-2 expression by WB (Fig. 4a) and IF (Fig. 4b). During DSS-induced colitis, claudin-1 was downregulated as expected. Importantly, this reduction was completely prevented in colitic mice
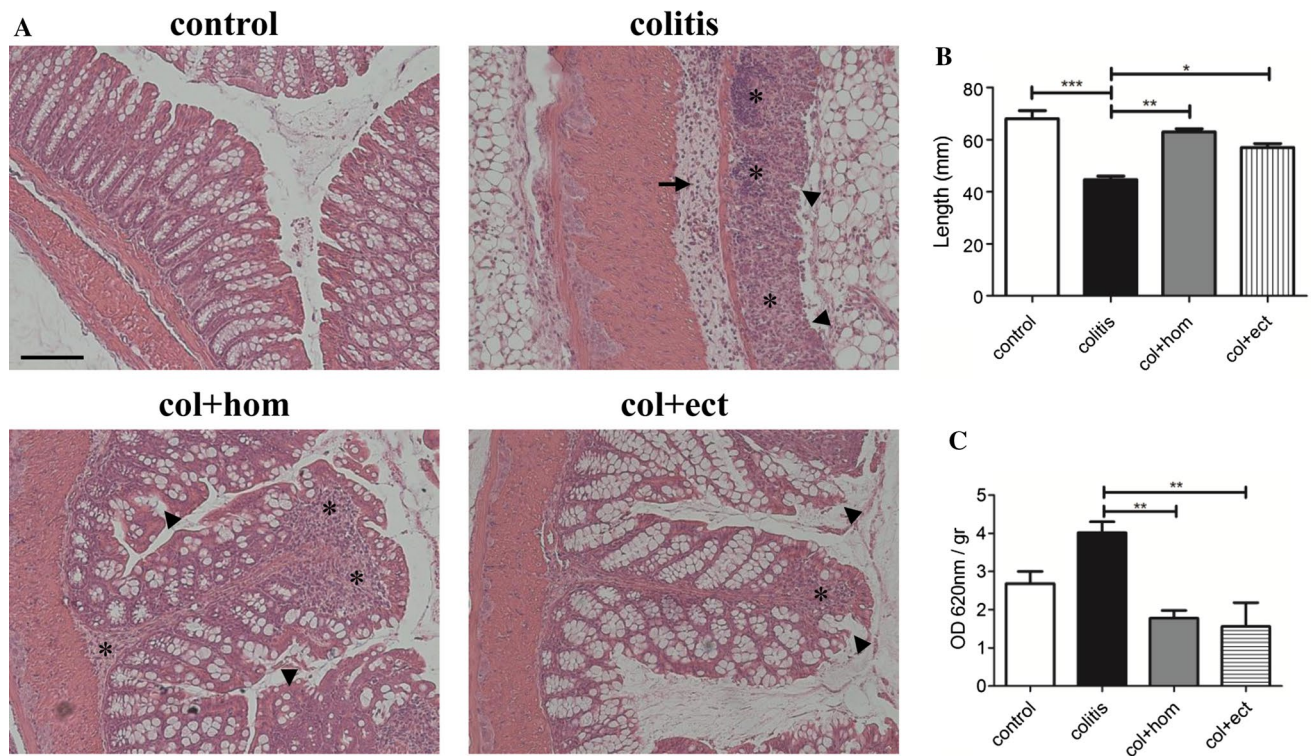
Fig. 3 DSS-induced tissue damage is less severe in animals co-treated with homoectoine or ectoine. DSS-colitis was induced in C57Bl/6 mice for 7 days. Homoectoine and ectoine treatments were administered daily by oral gavage in parallel to colitis induction. **a** Hematoxylin and eosin stainings of colon cross-sections show normal tissue morphology in control mice. During colitis edema formation (arrow), apical erosions (arrowheads) and immune cell recruitment (asterisks) can be seen. Less severe tissue alterations are observed in colitic ani-mals co-treated with homoectoine (col+hom) or ectoine (col+ect). Representative images of three independent experiments are shown (magnification ×40; bar = 50 μm). **b** Quantification of colon lengths. **c** Mouse colon permeability for Evans blue was measured in vivo in the four experimental groups: control, colitis, colitis+homoectoine (col+hom) and colitis+ectoine (col+ect). $n = 4$ per group in all experiments. Values are given as mean ± SDM. *$p < 0.05$, **$p < 0.01$, ***$p < 0.001$

Table 1 Histological inflammation scores

	Control	Colitis	Colitis + hom	Colitis + ect
Inflammation	0.4 ± 0.13	8.71 ± 0.85	4.1 ± 0.82***	5.05 ± 0.85***
Extent	0.4 ± 0.12	11.62 ± 0.26	1.65 ± 0.16***	7.6 ± 0.64***
Crypt damage	0.35 ± 0.1	14.1 ± 0.52	1.85 ± 0.22***	8.8 ± 1.03***
Total score	1.15 ± 0.12	34.43 ± 0.54	7.6 ± 0.4***	21.45 ± 0.84***

Hematoxylin and eosin staining of three independent tissue preparations were analyzed for the indicated parameters in the four experimental groups control, colitis, colitis+homoectoine (hom) and colitis+ectoine (ect). Values are mean ± SEM. ***$p < 0.001$ (respective treatment vs colitis)

treated with homoectoine. However, claudin-1 levels in colitic mice were not affected by ectoine. Claudin-2 was constitutively expressed at low levels in control groups and its expression was significantly upregulated during DSS-colitis. However, when colitic mice were treated with homoectoine or ectoine, claudin-2 levels were reduced to basal levels (Fig. 4a). IF images corroborated the WB results (Fig. 4b). Thus, complete prevention of this inflammatory claudin switch by homoectoine could explain its

stronger protective effect against inflammation (compare Table 1).

To test the effects of homoectoine and ectoine on the architecture of AJ, we analyzed the expression of E-cadherin and β-catenin in colon tissues of the four experimental groups. Interestingly, no significant changes on total protein levels were observed by western blot (Fig. 4c). IFs showed that E-cadherin and β-catenin localized to cell contacts in a similar fashion in all conditions (Fig. 4D).

Inflammatory Changes in TEER Are Ameliorated Only by Homoectoine, Whereas the Increase in Paracellular Flux Is Similarly Attenuated by Homoectoine and Ectoine

Given the different effects on claudins, we analyzed whether homoectoine and ectoine also had different effects on barrier dysfunction using Caco-2 cells as in vitro model of intestinal epithelial barrier. As expected, TEER was significantly lower in cells treated with the pro-inflammatory cytokines IFN-γ and TNF-α compared to untreated cells (Fig. 5a). Importantly, only homoectoine significantly ameliorated the drop in TEER. By contrast, both homoectoine and ectoine equally reduced excessive paracellular flux of 4 kDa FITC-dextran (Fig. 5b). This finding is in line with the WB data (Fig. 4A) showing that both compatible solutes prevented the reduction in occludin levels (regulation of macromolecular paracellular flux), whereas only homoectoine significantly prevented the reduction in claudin-1 (regulation of ion flux/resistance).

Expression of Inflammatory Mediators and Generation of Oxidative Stress Is Regulated by Ectoine and Homoectoine

The exacerbated production of pro-inflammatory cytokines and chemokines during colitis, contributes to neutrophil recruitment, tissue damage and excessive intestinal epithelial permeability [24]. Therefore, we analyzed mRNA production of key inflammatory mediators such as IFN-γ, TNF-α, IL1-β, KC and IL-10. During colitis KC, TNF-α, IL1-β and IFN-γ were significantly elevated compared to healthy mice. However, both ectoines had different effects on cytokine production (Fig. 6a). IFN-γ elevation was completely prevented by both ectoine and homoectoine, whereas TNF-α, KC and IL-1β production was only slightly decreased in homoectoine- and ectoine-treated mice. Production of the anti-inflammatory cytokine IL-10, which is increased in IBD patients during recovery phases [25], was also significantly increased in the colons of ectoine and homoectoine-treated mice.

Mucin 2 (MUC2) plays a critical role in epithelial protection [26]. Both MUC2 production [27] and secretion [28] is reduced in UC patients. Thus, we analyzed whether homoectoine and ectoine can also regulate MUC2 expression. Production of MUC2 mRNA in the colon was significantly reduced after DSS treatment, as expected. Of note, MUC2 mRNA levels in colons of ectoine- and homoectoine-treated mice were similar to control levels (Fig. 6a).

Excessive neutrophil recruitment is another important characteristic of colitis contributing to tissue damage [29]. As a consequence of neutrophil influx, production and release of reactive oxygen species (ROS) increase leading to oxidative stress. Thus, we analyzed the production of ROS in colon cross-sections of treated and untreated mice. During DSS-induced colitis, we observed a strong increase in oxidative stress, which was significantly prevented by both homoectoine and ectoine (Fig. 6b).

In summary, our data show clear protective effects of ectoine and homoectoine on various aspects of inflammatory tissue damage during colitis such as epithelial barrier dysfunction, pro-inflammatory mediator production, junction architecture and oxidative stress. While most effects were similarly pronounced with both ectoines; only homoectoine protected against loss of claudin-1 expression.

Discussion

Ectoine is a compatible solute produced by halophilic microorganisms in response to stressful stimuli that has anti-inflammatory properties in different model systems [8]. A recent study investigated the effects of ectoine during TNBS-colitis in rats. Administration of ectoine previous to the induction of colitis resulted in protection against weight loss, reduction of ulcerative areas in the colon, decrease in pro-inflammatory cytokine levels, reduced oxidative stress and tissue damage. However, it is unknown whether this is also the case in other species using different colitis-inducing agents; and effects of ectoine on epithelial barrier functions have never before been studied. Moreover, it is unknown whether synthetic ectoine derivatives such as homoectoine would have even stronger effects than ectoine.

DSS-colitis is a well-established experimental model in mice that resembles histopathological and clinical features observed in human IBD [30]. Our findings show that ectoine treatment during DSS-colitis significantly diminishes the DAI. Parallel administration of ectoine and DSS had a protective effect similar to the pre-treatment used in rats with TNBS-colitis [16]. In that study, ectoine was shown to ameliorate histopathological features of TNBS-colitis such as necrosis of the mucosa, edema formation and transmural infiltration in a manner similar to what was observed with sulfasalazine, a drug currently used for IBD treatment. In our model, ectoine treatment also led to reduction of edema formation, leukocyte infiltration, inflammation, and crypt damage. Nevertheless, it will be important to study whether the administration of ectoine and homoectoine as pre-treatment would have even stronger protective effects against DSS-colitis.

Nothing is known about potential effects of homoectoine during inflammation in general and colitis in particular. Our data now show that homoectoine was even more efficient in preventing tissue damage and inflammation than ectoine (compare Table 1 and Fig. 3). We observed similar results with homoectoine and ectoine in the protection
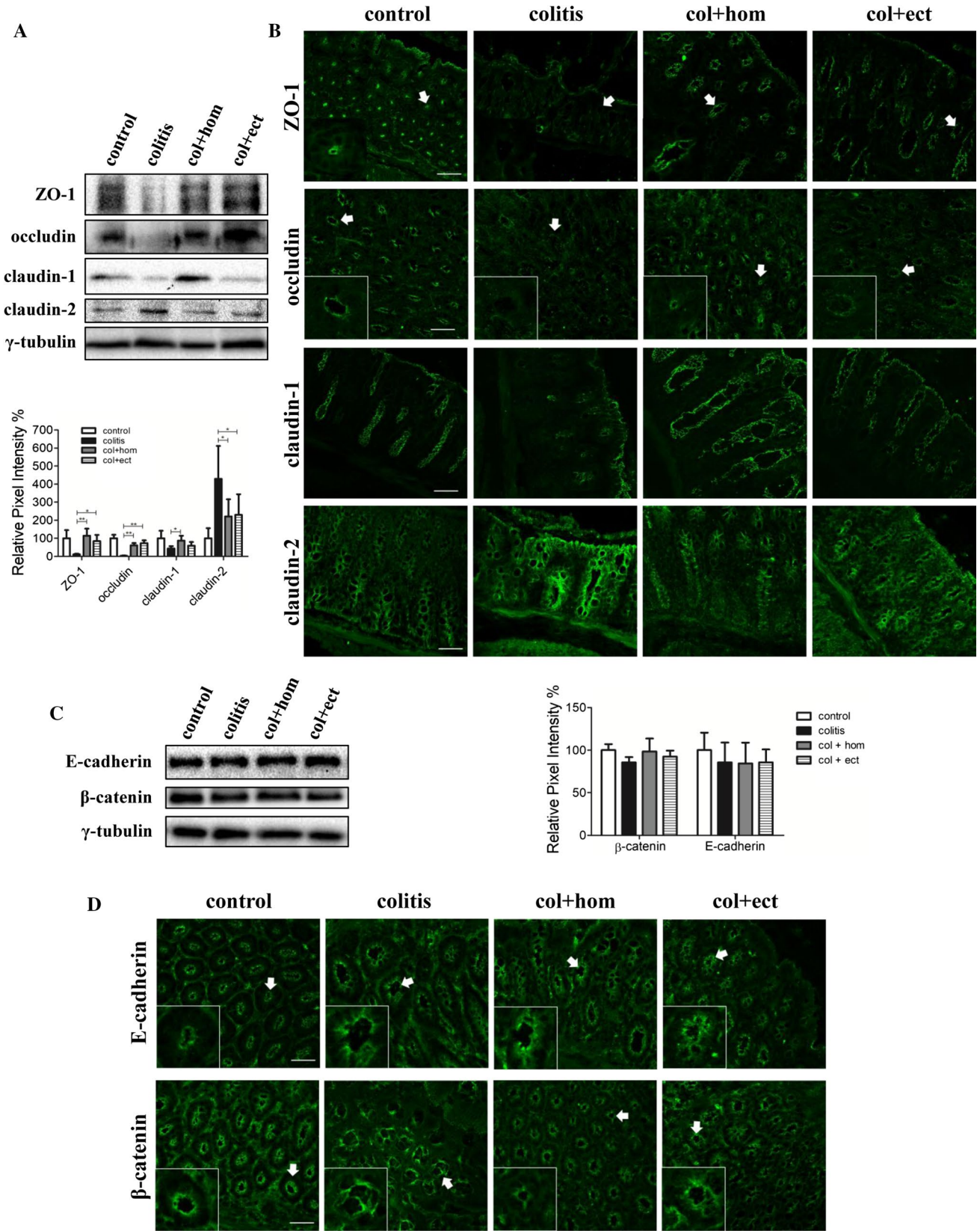
◄**Fig. 4** Colitis-induced disruption of TJ is ameliorated by homoectoine and ectoine. **a** WB of mouse colon lysates for ZO-1, occludin, claudin-1, claudin-2 and γ-tubulin of the four experimental groups: control, colitis, colitis + homoectoine (col + hom) and colitis + ectoine (col + ect). Bar graph represents quantification of pixel intensities of the respective protein bands normalized to γ-tubulin. **b** IF images of colon cross-sections stained for ZO-1, occludin, claudin-1 and claudin-2 of the four experimental groups. Arrows indicate apical crypt stainings (magnification ×40, bar = 50 μm). **c** WB of mouse colon lysates for E-cadherin, β-catenin and γ-tubulin of the four experimental groups. Bar graph represents quantification of pixel intensities of the respective protein bands normalized to γ-tubulin. No significant differences were detected. **d** IF images of colon cross-sections of the four experimental groups stained for E-cadherin, β-catenin. Arrows indicate apical crypt stainings (magnification: ×40, bar = 50 μm). $n = 3$ in all experiments. Quantification values given as mean ± SDM. *$p < 0.05$, **$p < 0.01$

against excessive epithelial permeability for Evans Blue in the colon. Using Caco-2 cells as in vitro model of intestinal epithelial barrier, the increase in paracellular flux of 4 kDa FITC–dextran induced by TNF-α and IFN-γ was equally prevented by both ectoines. However, when analyzing TEER as means to measure ion flux, we found that only homoectoine had a significant protective effect. Defects in epithelial barrier function have been observed during inflammatory disorders such as IBD [31]. Excessive intestinal permeability alone is not sufficient to induce IBD since asymptomatic first-degree relatives of IBD patients presented increased intestinal permeability without developing the disease [32]. Moreover, mice deficient for cortactin or non-muscle myosin IIA heavy chain show increased basal epithelial permeability in the colon, but did not develop spontaneous colitis [4, 33]. However, increased permeability aggravates clinical symptoms of IBD. Intercellular junctions that regulate permeability are destabilized by pro-inflammatory stimuli.

For example, IFN-γ induces internalization of epithelial TJ proteins [34]; immune cells such as dendritic cells open TJ in order to sample bacteria in the lumen [35]; and pathogens induce the production of proinflammatory cytokines and release proteases that cleave junction proteins [36]. Disruption of junctions leads to altered ion and macromolecule fluxes and an increased passage of antigens of the lumen microbiota, thus triggering the inflammatory response. ZO-1, occludin and the family of claudins are key components of the TJ that regulate barrier integrity. ZO-1 is an intercellular protein essential for TJ stability and barrier functions for solutes [37], and it binds to the transmembrane proteins occludin and claudins linking them to the actin cytoskeleton. Occludin is mainly involved in the regulation of paracellular flux of 4 kDa FITC-dextran, whereas claudins permit the selective flux of ions across the barrier [38]. During DSS-colitis, occludin and ZO-1 levels are significantly reduced until their complete depletion [39]. However, effects are not as clear with claudin-1 expression during DSS-colitis [17, 40]. Our findings show a clear loss of ZO-1, occludin and claudin-1 during DSS-colitis. Both homoectoine and ectoine prevented the downregulation of ZO-1 and occludin. By contrast, rescue of claudin-1 expression during colitis was only observed with homoectoine, but not with ectoine. On the other hand, claudin-2 forms selective pores for small ions and is expressed mostly in leaky epithelia [41]. During colitis, claudin-2 expression is upregulated in the colon [42], which we could confirm in this study. Of note, both ectoine and homoectoine significantly inhibited the increase in claudin-2 during colitis. These data provide an explanation for our results that only homoectoine had a protective effect against increased ion flux (controlled by claudins); and that both ectoine and homoectoine similarly reduced paracellular
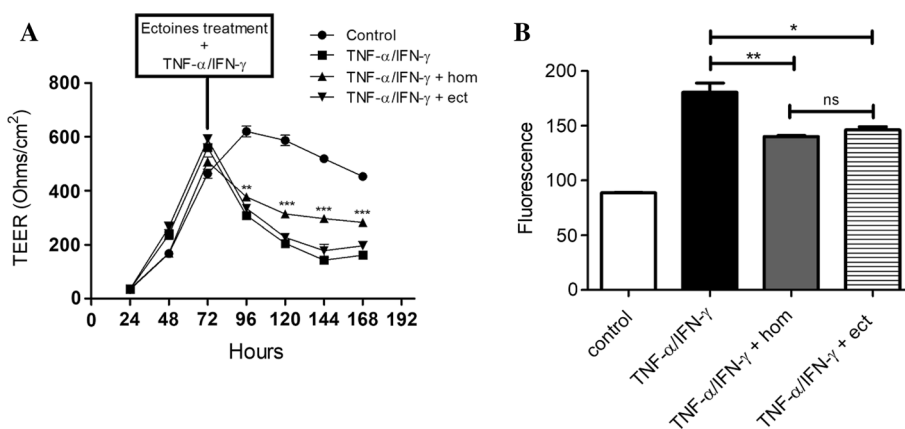

Fig. 5 Increased epithelial permeability during inflammation is attenuated by homoectoine and ectoine in vitro. **a** Transepithelial electrical resistance (TEER) across confluent Caco-2 monolayers grown on 0.4 μm filters was measured every 24 h. Once cultures reached confluence, they received an inflammatory stimulus with 100U/ml IFN-γ and 5 nM TNF-α. In parallel, they were treated with 1 mM ectoine, 1 mM homoectoine or left untreated. **b** Once TEER was established, flux of 4 kDa FITC-dextran was measured fluorometrically at 488 nm after 24-h incubation. $n = 4$ in all experiments. Values are given as mean ± SDM. *$p < 0.05$, **$p < 0.01$, ***$p < 0.001$
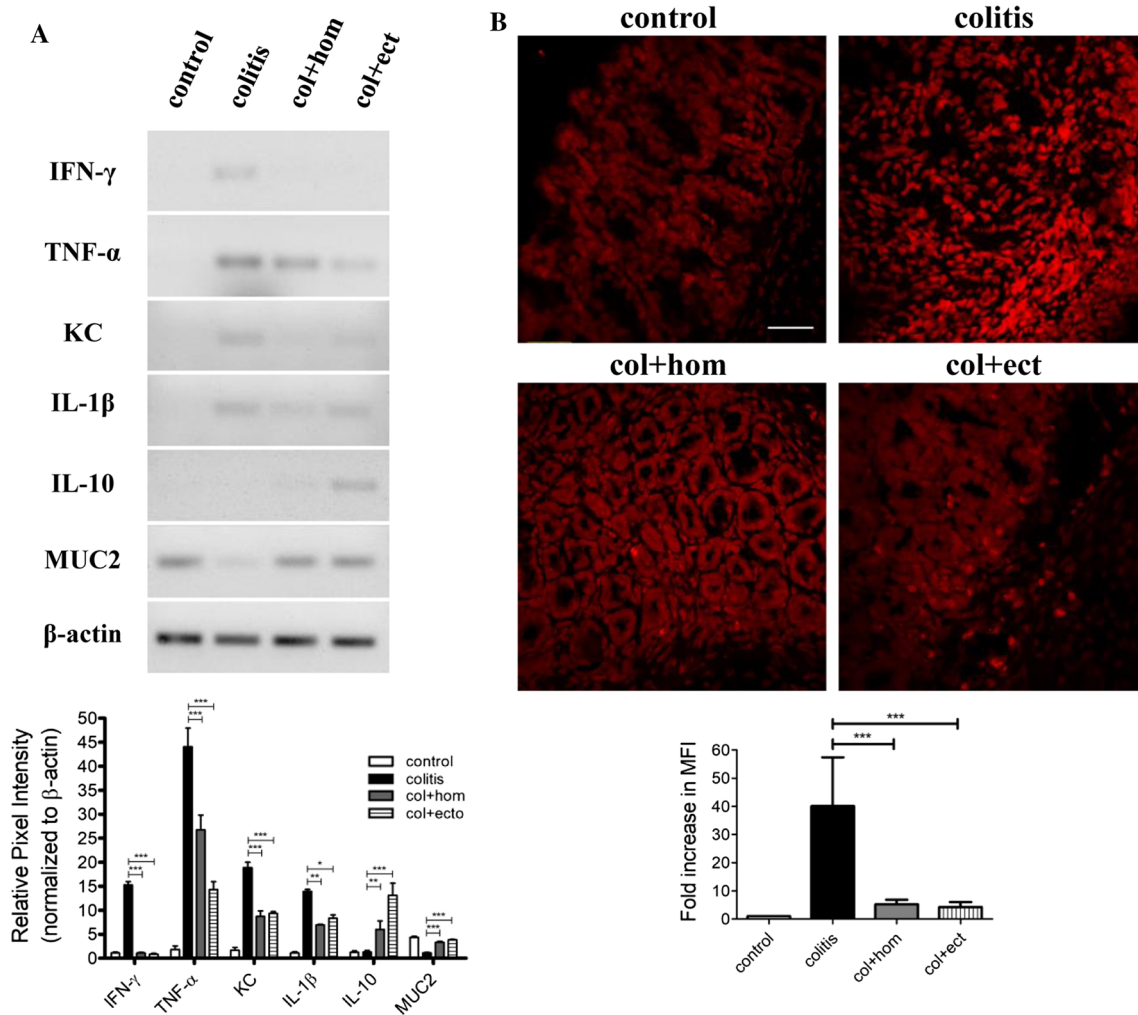
Fig. 6 Treatment with homoectoine or ectoine reduces the production of pro-inflammatory cytokines and oxidative stress during colitis. **a** RT-PCR of cDNA derived from mouse colons of the four experimental groups: control, colitis, colitis+homoectoine (col+hom) and colitis+ectoine (col+ect) for the indicated cytokines/chemokines, and mucin-2. β-actin served as house-keeping gene. The bar graph represents quantification of pixel intensities of the respective cytokine bands normalized to β-actin. Representative images of three inde-

pendent experiments, $n = 3$ in each group. **b** Colon cross-sections of the four experimental groups were incubated with 5 μM dihydroethidium (DHE) as described in methods. Representative fluorescent images of oxidized ethidium are shown. The bar graph shows fold increase of mean fluorescence intensity (MFI) normalized to the control group. $n = 3$ in each group. Bar = 50 μm. *$p < 0.05$; **$p < 0.01$; ***$p < 0.001$

flux of 4 kDa FITC-dextran (controlled by occludin). Our data clearly demonstrate that the compatible solutes ectoine and especially homoectoine protect epithelial junction architecture during colitis, thus contributing to the maintenance of intestinal barrier integrity. It will be interesting in the future to analyze potential protective effects of ectoines during the recovery phase after acute colitis and during chronic experimental colitis after several cycles of DSS treatment. Moreover, during severe inflammatory disorders such as sepsis, intestinal barrier dysfunction characterized by excessive permeability contributes to the development of organ dysfunction syndrome [43]. Therefore, it will be important

to determine whether these compatible solutes can prevent intestinal barrier hyperpermeability during sepsis.

Ectoine regulated the expression of pro-inflammatory cytokines during TNBS-induced colitis in rats [16]. Here, we show that both homoectoine and ectoine reduce the production of IFN-γ, TNF-α, KC, IL1-β and promote production of the anti-inflammatory cytokine IL-10. Moreover, we observed that both homoectoine and ectoine reduced oxidative stress in colon tissues from colitic mice probably due to ROS scavenging activity. This is in line with previous reports showing that ectoine had antioxidative properties in human skin cells [10]; and with the fact that neutrophils

are recruited during DSS-colitis into the colon where they release proteases and ROS that contribute to tissue damage [44].

Taken together, our data suggest that homoectoine and ectoine ameliorate tissue damage induced by DSS-colitis by reducing the inflammatory response and stabilizing intestinal epithelial junctions. Due to the complete prevention of the colitis-induced claudin switch, homoectoine most likely has a stronger protective effect during colitis. The exact molecular mechanisms require further investigation, but could be related to the stabilization of proteins and membranes and prevention of water loss according to the preferential exclusion model [21]. Ectoine is currently used for the treatment of allergic rhinitis [45], conjunctivitis and atopic dermatitis [46]. Our results unequivocally show that ectoine and even more homoectoine protect against DSS-colitis. Importantly, homoectoine and ectoine did not cause any side effects in healthy mice. Thus, especially homoectoine has the potential to serve as beneficial diet supplement for IBD patients to reach or extend phases of remission.

Compliance with ethical standards

Conflict of interest The authors declare no conflict of interest.

References

1. Zhang YZ, Li YY. Inflammatory bowel disease: pathogenesis. *World J Gastroenterol.* 2014;20:91–99.
2. Abraham C, Cho JH. Inflammatory bowel disease. *N Engl J Med.* 2009;361:2066–2078.
3. Turner JR. Molecular basis of epithelial barrier regulation: from basic mechanisms to clinical application. *Am J Pathol.* 2006;169:1901–1909.
4. Citalan-Madrid AF, Vargas-Robles H, Garcia-Ponce A, et al. Cortactin deficiency causes increased RhoA/ROCK1-dependent actomyosin contractility, intestinal epithelial barrier dysfunction, and disproportionately severe DSS-induced colitis. *Mucosal Immunol.* 2017;10:1237–1247.
5. Triantafillidis JK, Merikas E, Georgopoulos F. Current and emerging drugs for the treatment of inflammatory bowel disease. *Drug Des Devel Ther.* 2011;5:185–210.
6. Troncone E, Monteleone G. The safety of non-biological treatments in Ulcerative Colitis. *Expert Opin Drug Saf.* 2017;16:779–789.
7. Galinski EA, Pfeiffer HP, Truper HG. 1,4,5,6-Tetrahydro-2-methyl-4-pyrimidinecarboxylic acid. A novel cyclic amino acid from halophilic phototrophic bacteria of the genus *Ectothiorhodospira*. *Eur J Biochem.* 1985;149:135–139.
8. Pastor JM, Salvador M, Argandona M, et al. Ectoines in cell stress protection: uses and biotechnological production. *Biotechnol Adv.* 2010;28:782–801.
9. Smiatek J, Harishchandra RK, Rubner O, Galla HJ, Heuer A. Properties of compatible solutes in aqueous solution. *Biophys Chem.* 2012;160:62–68.
10. Buenger J, Driller H. Ectoin: an effective natural substance to prevent UVA-induced premature photoaging. *Skin Pharmacol Physiol* 2004;17:232–237.
11. Sydlik U, Gallitz I, Albrecht C, Abel J, Krutmann J, Unfried K. The compatible solute ectoine protects against nanoparticle-induced neutrophilic lung inflammation. *Am J Respir Crit Care Med.* 2009;180:29–35.
12. Abdel-Aziz H, Wadie W, Scherner O, Efferth T, Khayyal MT. Bacteria-derived compatible solutes ectoine and 5alpha-hydroxyectoine act as intestinal barrier stabilizers to ameliorate experimental inflammatory bowel disease. *J Nat Prod.* 2015;78:1309–1315.
13. Schnoor M, Voss P, Cullen P, et al. Characterization of the synthetic compatible solute homoectoine as a potent PCR enhancer. *Biochem Biophys Res Commun.* 2004;322:867–872.
14. Sauer T, Galinski EA. Bacterial milking: a novel bioprocess for production of compatible solutes. *Biotechnol Bioeng.* 1998;59:128.
15. Koichi M, Mitsuhiko M, Tatsuo N, Yoshio S. Production of tetrahydropyrimidine derivatives. Japanese Patent Application JPH3031265A; 1991.
16. Abdel-Aziz H, Wadie W, Abdallah DM, Lentzen G, Khayyal MT. Novel effects of ectoine, a bacteria-derived natural tetrahydropyrimidine, in experimental colitis. *Phytomedicine.* 2013;20:585–591.
17. Mennigen R, Nolte K, Rijcken E, et al. Probiotic mixture VSL#3 protects the epithelial barrier by maintaining tight junction protein expression and preventing apoptosis in a murine model of colitis. *Am J Physiol Gastrointest Liver Physiol.* 2009;296:G1140–1149.
18. Mendoza MG, Castillo-Henkel C, Medina-Santillan R, et al. Kidney damage after renal ablation is worsened in endothelial nitric oxide synthase -/- mice and improved by combined administration of L-arginine and antioxidants. *Nephrol (Carlton).* 2008;13:218–227.
19. Viennois E, Chen F, Laroui H, Baker MT, Merlin D. Dextran sodium sulfate inhibits the activities of both polymerase and reverse transcriptase: lithium chloride purification, a rapid and efficient technique to purify. *RNA BMC Res Notes.* 2013;6:360.
20. Sydlik U, Peuschel H, Paunel-Gorgulu A, et al. Recovery of neutrophil apoptosis by ectoine: a new strategy against lung inflammation. *Eur Respir J.* 2013;41:433–442.
21. Graf R, Anzali S, Buenger J, Pfluecker F, Driller H. The multifunctional role of ectoine as a natural cell protectant. *Clin Dermatol.* 2008;26:326–333.
22. Gersemann M, Becker S, Kubler I, et al. Differences in goblet cell differentiation between Crohn's disease and ulcerative colitis. *Differentiation.* 2009;77:84–94.
23. Hering NA, Fromm M, Schulzke JD. Determinants of colonic barrier function in inflammatory bowel disease and potential therapeutics. *J Physiol.* 2012;590:1035–1044.
24. Onyiah JC, Colgan SP. Cytokine responses and epithelial function in the intestinal mucosa. *Cell Mol Life Sci.* 2016;73:4203–4212.
25. Mitsuyama K, Tomiyasu N, Takaki K, et al. Interleukin-10 in the pathophysiology of inflammatory bowel disease: increased serum concentrations during the recovery phase. *Med Inflamm.* 2006;2006:26875.
26. Van der Sluis M, De Koning BA, De Bruijn AC, et al. Muc2-deficient mice spontaneously develop colitis, indicating that MUC2 is critical for colonic protection. *Gastroenterology.* 2006;131:117–129.

27. Tytgat KM, van der Wal JW, Einerhand AW, Buller HA, Dekker J. Quantitative analysis of MUC2 synthesis in ulcerative colitis. *Biochem Biophys Res Commun.* 1996;224:397–405.
28. Van Klinken BJ, Van der Wal JW, Einerhand AW, Buller HA, Dekker J. Sulphation and secretion of the predominant secretory human colonic mucin MUC2 in ulcerative colitis. *Gut* 1999;44:387–393.
29. Parkos CA. Neutrophil-epithelial interactions: a double-edged sword. *Am J Pathol.* 2016;186:1404–1416.
30. Perse M, Cerar A. Dextran sodium sulphate colitis mouse model: traps and tricks. *J Biomed Biotechnol.* 2012;2012:718617.
31. Salim SY, Soderholm JD. Importance of disrupted intestinal barrier in inflammatory bowel diseases. *Inflamm Bowel Dis.* 2011;17:362–381.
32. Halme L, Paavola-Sakki P, Turunen U, Lappalainen M, Farkkila M, Kontula K. Family and twin studies in inflammatory bowel disease. *World J Gastroenterol.* 2006;12:3668–3672.
33. Naydenov NG, Feygin A, Wang D, et al. Nonmuscle Myosin IIA Regulates Intestinal Epithelial Barrier in vivo and Plays a Protective Role During Experimental Colitis. *Sci Rep.* 2016;6:24161.
34. Bruewer M, Utech M, Ivanov AI, Hopkins AM, Parkos CA, Nusrat A. Interferon-gamma induces internalization of epithelial tight junction proteins via a macropinocytosis-like process. *FASEB J.* 2005;19:923–933.
35. Rescigno M, Urbano M, Valzasina B, et al. Dendritic cells express tight junction proteins and penetrate gut epithelial monolayers to sample bacteria. *Nat Immunol.* 2001;2:361–367.
36. Nava P, Kamekura R, Nusrat A. Cleavage of transmembrane junction proteins and their role in regulating epithelial homeostasis. *Tissue Barriers.* 2013;1:e24783.
37. Van Itallie CM, Fanning AS, Bridges A, Anderson JM. ZO-1 stabilizes the tight junction solute barrier through coupling to the perijunctional cytoskeleton. *Mol Biol Cell.* 2009;20:3930–3940.
38. Steed E, Balda MS, Matter K. Dynamics and functions of tight junctions. *Trends Cell Biol.* 2010;20:142–149.
39. Poritz LS, Garver KI, Green C, Fitzpatrick L, Ruggiero F, Koltun WA. Loss of the tight junction protein ZO-1 in dextran sulfate sodium induced colitis. *J Surg Res.* 2007;140:12–19.
40. Iraha A, Chinen H, Hokama A, et al. Fucoidan enhances intestinal barrier function by upregulating the expression of claudin-1. *World J Gastroenterol.* 2013;19:5500–5507.
41. Amasheh S, Meiri N, Gitter AH, et al. Claudin-2 expression induces cation-selective channels in tight junctions of epithelial cells. *J Cell Sci.* 2002;115:4969–4976.
42. Ahmad R, Chaturvedi R, Olivares-Villagomez D, et al. Targeted colonic claudin-2 expression renders resistance to epithelial injury, induces immune suppression, and protects from colitis. *Mucosal Immunol.* 2014;7:1340–1353.
43. Yoseph BP, Klingensmith NJ, Liang Z, et al. Mechanisms of intestinal barrier dysfunction in sepsis. *Shock.* 2016;46:52–59.
44. Damiani CR, Benetton CA, Stoffel C, et al. Oxidative stress and metabolism in animal model of colitis induced by dextran sulfate sodium. *J Gastroenterol Hepatol.* 2007;22:1846–1851.
45. Werkhauser N, Bilstein A, Sonnemann U. Treatment of allergic rhinitis with ectoine containing nasal spray and eye drops in comparison with azelastine containing nasal spray and eye drops or with cromoglycic acid containing nasal spray. *J Allergy (Cairo).* 2014;2014:176597.
46. Marini A, Reinelt K, Krutmann J, Bilstein A. Ectoine-containing cream in the treatment of mild to moderate atopic dermatitis: a randomised, comparator-controlled, intra-individual double-blind, multi-center trial. *Skin Pharmacol Physiol.* 2014;27:57–65.

Affiliations

Karla F. Castro-Ochoa[1] · Hilda Vargas-Robles[1] · Sandra Chánez-Paredes[1] · Alfonso Felipe-López[1,6] · Rodolfo I. Cabrera-Silva[1] · Mineko Shibayama[2] · Abigail Betanzos[2,3] · Porfirio Nava[4] · Erwin A. Galinski[5] · Michael Schnoor[1]

Karla F. Castro-Ochoa
ktzala@gmail.com

Hilda Vargas-Robles
hildavargasr@yahoo.com.mx

Sandra Chánez-Paredes
schanezp@gmail.com

Alfonso Felipe-López
alfonso.felipe@cinvestav.mx

Rodolfo I. Cabrera-Silva
cabreraismael2@gmail.com

Mineko Shibayama
mineko@cinvestav.mx

Abigail Betanzos
abetanzos@cinvestav.mx

Porfirio Nava
pnava@fisio.cinvestav.mx

Erwin A. Galinski
galinski@uni-bonn.de

[1] Department of Molecular Biomedicine, CINVESTAV, Avenida IPN 2508, San Pedro Zacatenco, 07360 Mexico-City, Mexico

[2] Department of Infectomics and Molecular Pathogenesis, CINVESTAV, Avenida IPN 2508, San Pedro Zacatenco, 07360 Mexico-City, Mexico

[3] Conacyt, Av. Insurgentes Sur 1582, 03940 Mexico-City, Mexico

[4] Department of Physiology, Biophysics and Neurosciences, CINVESTAV, Avenida IPN 2508, San Pedro Zacatenco, 07360 Mexico-City, Mexico

[5] Institute of Microbiology and Biotechnology, University of Bonn, 53115 Bonn, Germany

[6] Present Address: Molecular Biology Division, Navy Medical Center, Ministry of Marine and Army, Av. Heroica Escuela Naval Militar, 04470 Mexico-City, Mexico